Electrochimica Acta 269 (2018) 610–616

Contents lists available at ScienceDirect

Electrochimica Acta

journal homepage: www.elsevier.com/locate/electacta

Electrochemically controllable coating of a functional silicon film on carbon materials

Hongwei Xie [a], Haijia Zhao [a], Jinyun Liao [b], Huayi Yin [a,*], Allen J. Bard [b]

[a] School of Metallurgy, Northeastern University, Shenyang 110819, PR China
[b] Center for Electrochemistry, Department of Chemistry and Biochemistry, The University of Texas at Austin, TX 78712, USA

ARTICLE INFO

Article history:
Received 27 December 2017
Received in revised form
1 March 2018
Accepted 1 March 2018
Available online 2 March 2018

Keywords:
Silicon film
Electrodeposition
Molten salts
Carbon substrate
Anode materials

ABSTRACT

A silicon deposit of various forms was successfully coated on graphite by electrodeposition in molten $CaCl_2$ containing nano-SiO_2 as a silicon precursor. The morphologies of the deposited silicon can be tuned from Si nanowires to a dense film by controlling constant electrolysis cell voltage. In addition to controlling electrochemical polarizations, the substrate plays a key role in forming a dense silicon film. By analyzing the interface between the Si film and graphite substrate, a thin transition layer comprising of Si, SiC and C enables the good adhesion of the Si film with the carbon substrate and thereby helps the growth of a dense Si film. Besides the application for photovoltaics, the electrolytic p-type Si film was employed as a binder-free anode for lithium-ion batteries delivering a capacity of over 2500 mAh g^{-1} in the first 10 cycles and retaining 800 mAh g^{-1} after 40 cycles. Moreover, this method was applied for coating Si on carbon fibers, which could be a general way to prepare Si with controllable forms and silicon/carbon core-shell structures for functional materials.

1. Introduction

Silicon (Si) is a major and indispensable functional material used in photovoltaics, electronics, and energy conversion and storage devices in our daily life [1–6]. For example, Si solar cell accounts for more 95% of the whole solar cell market. Moreover, Si is a promising anode candidate of a theoretical capacity around 4200 mAh g^{-1} in lithium-ion batteries (LIBs), an order of magnitude higher than that of graphite [7,8]. Prior to practical applications, the metallurgical silicon produced by carbothermal reduction is firstly purified, and then the purified silicon is made into various forms, i.e., thin films, sheets, nanowires, nanotubes, nanoparticles, and etc. Usually, the manufacturing steps consume a huge amount of energy, possess a low material utilization, need elaborate equipment, and strict synthetic conditions. Therefore, a low-cost and short-process approach for preparing functional Si materials is of great interest.

Electrochemical deposition of Si in non-aqueous electrolytes, like organic solvents [9,10], room temperature ionic liquids [11] and high-temperature molten salts [12–18], has been demonstrated to be a straightforward way. Due to the poor electronic conductance of Si at room temperature, only a very thin layer of Si deposit could be prepared. By contrast, the electronic conductivity of Si is several orders of magnitude higher at high temperature than that at room temperature, which is advantageous to reduce the overpotential and then enables a continuous growth of Si. Since 2000, direct electrochemical reduction of solid oxides including SiO_2 in molten $CaCl_2$ has been proved to be an energy-efficient approach to producing Si [19–26]. Electrochemical deposition of Si on a Ag foil substrate in molten $CaCl_2$ containing nano-SiO_2 was recently reported [27]. The as-received porous Si deposit exhibited photo-response and Ag substrate played a key role in catalyzing the growth of Si. Considering the high cost of Ag, replacing Ag by a low-cost substrate was used for depositing Si film as well [28,29]. Moreover, the deposited Si film was in-situ doped, and the thickness of Si was increased by adding CaO into molten $CaCl_2$ [29]. It has been observed that it is more difficult to prepare dense Si film on metal substrates (i.e., Mo, Ni, Ag) than that in carbon substrate in molten $CaCl_2$ [24,27,30], while a dense Si film was prepared on Ag substrate in molten KCl-KF with K_2SiF_6 as Si precursor [18]. From a thermodynamic viewpoint, carbon could spontaneously react with Si to generate SiC, and SiC has a large band gap of ~3.0eV, which could cause high polarization during electrolysis and photoelectrochemical (PEC) test. However, no big polarization was observed in both electrolysis and PEC measurements, and few studies reported the reaction of Si with

* Corresponding author.
E-mail address: yinhy@smm.neu.edu.cn (H. Yin).

https://doi.org/10.1016/j.electacta.2018.03.002
0013-4686/

carbon at their interface. Therefore, it is worthwhile to investigate the boundary of Si/C which is helpful to understand the effect of substrate on the electrochemical deposition of Si in molten salts.

It is noted that the morphologies of Si deposition vary with varying the electrolysis potentials or current densities, and the carbon substrate is key to enabling the growth of a dense Si film. In addition, carbon-silicon hybrid materials attract extensive attention as a silicon-based anode in LIBs [5]. Inspired by the good adhesion of Si deposit with carbon substrate in our experiment, the interface of the electrolytic silicon and carbon is supposed to enhance the combination of the silicon layer with carbon substrate. Thus, the knowledge of the interaction between electrolytic silicon and carbon is crucial to understand the synergetic effect of carbon-silicon materials in various forms such as core-shell structure, coating, and decorations, especially at elevated temperatures.

In this paper, we present a one-step approach for depositing a p-type Si film on graphite foil and carbon fibers. The reduction process of SiO_2 precursor in $CaCl_2$ melt was investigated by cyclic voltammetry (CV), the effect of the cell voltages on the morphologies of the Si deposit was studied, and the interface of Si/C was investigated as well. In addition, the lithium storage performance of the as-received Si film was studied by CV and galvanostatic charge-discharge measurements.

2. Experimental

2.1. Cyclic voltammetry and electrolysis

All high-temperature experiments were performed in a quartz test vessel protected with Ar gas flow, and the test vessel was heated by a tube furnace. Cyclic voltammetry was performed using a three-electrode setup which was contained in an alumina crucible with 49.5 g $CaCl_2$ and 0.5 g SiO_2 nanoparticles (99.9%, 5–15 nm in diameter, Alfa Aesar). Graphite rods (˃99.999%, all from Alfa Aesar) served as the working electrode (1 mm in diameter), pseudo-reference electrode (3 mm in diameter) and counter electrode (6 mm in diameter), respectively. The nano-SiO_2 coated graphite working electrode was prepared by a dip-coating approach in an ethanol solution (0.1 g nano-SiO_2 (5–15 nm in diameter) dispersed in 10 mL ethanol). Before electrochemical measurement, $CaCl_2$ and SiO_2 were dried under vacuum at 250 °C for 24 h. Then the temperature of the furnace was ramped to melt the salt at 850 °C. Constant cell voltage electrolysis was conducted between a graphite foil cathode (surface area: 2 cm^2, Alfa Aesar) and a graphite rod anode in the same melt that used for CV measurement. After electrolysis, the graphite cathode was lifted out from the melt and cooled down in the headspace of the quartz test vessel. Afterward, the sample was taken out from the test vessel and washed with water to remove the salt away from the sample. Finally, the deposit was vacuum-dried at 120 °C for 10 h before characterization. The same electrochemical deposition process was conducted in the same melt on a carbon fiber electrode.

2.2. Photoelectrochemical measurement

The PEC measurement was performed in an acetonitrile solution containing 0.1 mol L^{-1} tetrabutylammonium hexafluorophosphate ($TBAF_6$, Fluka, Allentown, PA) as supporting electrolyte and 0.05 mol L^{-1} ethyl viologen diperchlorate (EV^{2+}, Sigma-Aldrich, St. Louis, MO) as redox reagent. A three-electrode setup was used to measure the voltage response of the as-prepared Si film. A platinum foil and a silver wire were employed as a counter electrode and a quasi-reference electrode, respectively. A Xe lamp of an incident light intensity of 100 mW cm^{-2} acted as a UV–visible light to irradiate the obtained Si film working electrode.

2.3. Electrochemical performances of Li storage

A half-cell was assembled to characterize the electrochemical performance of the electrolytic Si film working electrode coupled with a lithium foil acting counter electrode, and EC/DMC dissolved 1 M $LiPF_6$ was used as an electrolyte. For CV measurement, the lithium foil acts both reference and counter electrodes, and the measurement was controlled by a CHI660 electrochemical workstation. Galvanostatic charge-discharge was performed by a battery testing machine (Arbin, BT-2000).

2.4. Materials characterization

The electrolytic Si films were characterized by scanning electron microscopy (SEM, Quanta 650 FEG, FEI Company, Inc.) equipped an X-ray gun for energy dispersive spectroscopy (EDS, XFlash-Detector 5010, Bruker), transmission electron microscopy (TEM, JEM2010-HT), X-ray photoelectron spectroscopy (XPS, Kratos Analytical Ltd., UK), X-ray diffraction spectroscopy (XRD, Philips X-ray diffractometer equipped with Cu Kα radiation), time-of-flight secondary-ion mass spectroscopy (TOF-SIMS, Perkin-Elmer, Model ULVAC-PHI TFS2000 system equipped with a Bi-ion source).

3. Results and discussion

3.1. Characterization of electrolytic silicon

Electrochemical deposition of Si under a variety of potentials in molten $CaCl_2$–SiO_2 was conducted. The use of nano-SiO_2 coated graphite-rod working electrode is an effective way to characterize the electrochemical reduction of SiO_2. In the CV measurement, the coated SiO_2 on the working electrode was reduced corresponding to reduction peaks in the cyclic voltammograms. The reduction peak c4 is due to the reduction of SiO_2 coated on the surface of graphite electrode (Fig. 1a), which agrees well with the data reported by using a Si wafer electrode [22]. Two symmetrical pairs of redox peaks (c3/a3 and c4/a4) correspond to the alloy-dealloy reactions of Ca–Si alloys (Fig. 1a). To achieve the generation of Si, the applied potential of electrolysis should be controlled in a proper range. For example, in molten $CaCl_2$-1wt% SiO_2, a cell voltage from 1.8 to 2.6 V should be applied to prepare the pure Si (Fig. 1b and d), supposing the potential polarization on the anode is stable in a two-electrode electrolysis cell. Unlike the three-electrode cell employing SiO_2 coated working electrode, the bare carbon cathode was applied as a substrate in the two-electrode electrolysis cell, and Si deposit comes from reducing the nano-SiO_2 dispersed in molten $CaCl_2$. It is noted that Si deposits show different colors and forms, for example, the deposits obtained from 1.8 to 2.2 V are yellowish and powdery, and gray dense films were obtained at 2.4v and 2.6 V (Fig. 1c). From the XRD patterns (Fig. 1d), the diffraction peaks were sharper when the electrolysis voltage was increased from 1.8 to 2.6 V, indicating that the crystallinity or particle size of the electrolytic Si increased with increasing cell voltage (FWHMs (full width at half maximum) of the strongest peak are 0.55 and 0.35 for the sample obtained at 1.8 and 2.6 V, respectively).

To further analyze the Si deposits, the morphologies of the deposits were characterized by SEM and TEM, as shown in Fig. 2. Without deposition, graphite substrate was smooth (Fig. 2a), and Si nanowires were obtained under a constant cell voltage of 1.8 V and 2.0 V (Fig. 2b and c). At 2.2 V, the deposit was a mixture of Si particles and wires (Fig. 2d), and Si wires disappeared but a rough surface was observed when the cell voltage increased to 2.4 V and 2.6 V. In more detail, the diameter of Si nanowires is between 50 and 100 nm, and the Si wires obtained at 1.8 V are more straight

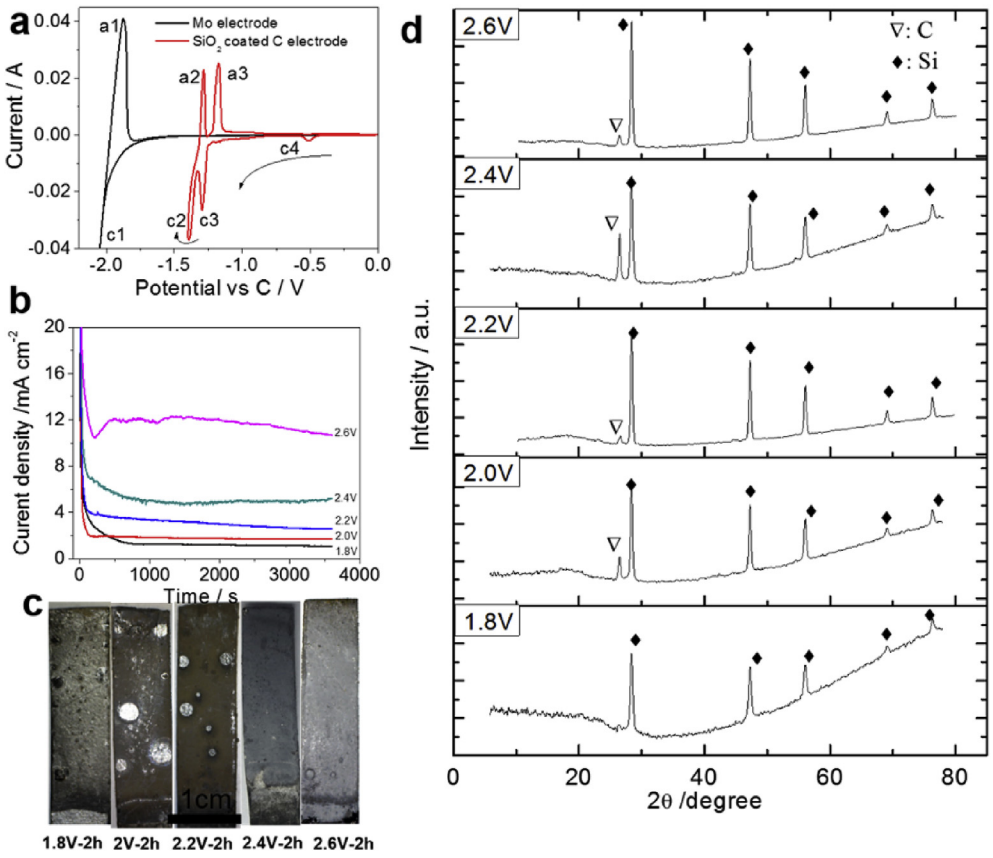

Fig. 1. (a) CVs recorded from Mo electrode and a nano-SiO_2 coated graphite electrode in pure $CaCl_2$ melt at 850 °C; (b) Current-time profiles recorded under indicated constant cell voltages; (c) digital pictures of Si deposits under indicated cell voltages; (d) XRD patterns of the Si deposits.

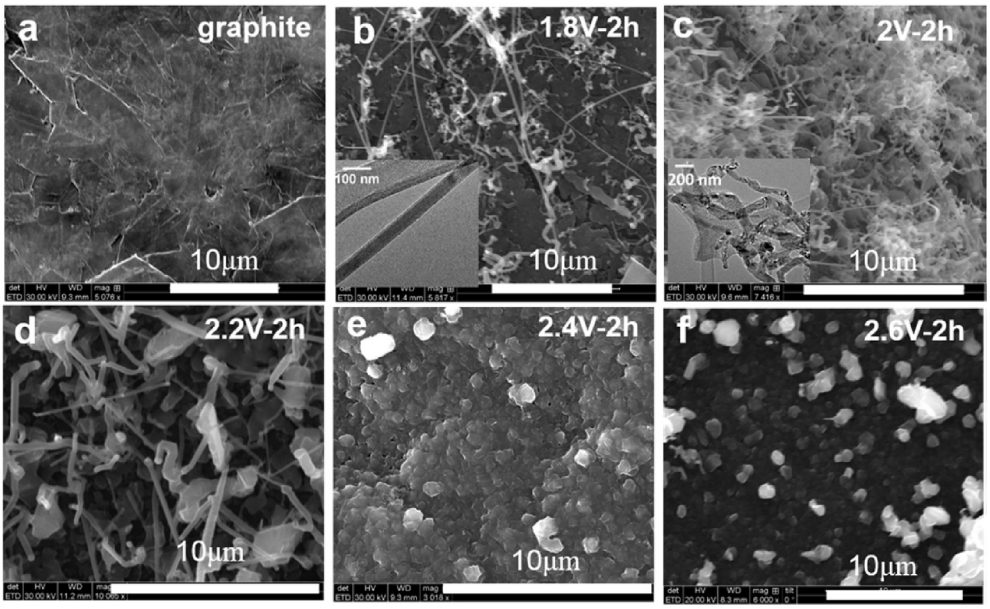

Fig. 2. SEM images of graphite foil (a) and the deposited Si obtained from 1.8 V to 2.6 V (the plateau current densities are 1, 2, 3, 6 and 10 mA cm^{-2}) for 2 h (b–f), their corresponding TEM images are inserted in b and c.

than that obtained at 2.0 V (the inset TEM images of Fig. 2b and c). At 2.0 V, the nanowires are tangled, and the diameter of Si wires grows up to 500 nm at 2.2 V. Therefore, the morphologies of Si deposits are controllable by controlling the electrolysis cell voltage. Similar effects of potential on the morphologies of the electrolytic products were observed in the electrochemical reduction of solid SiO_2, GeO_2, SiO_2/C to prepare semiconductors, like Si, Ge, and SiC nanowires, in molten salts [31–35]. But this phenomenon is rarely

observed for the electrochemical preparation of transition metals, like Fe, Ni, Cr, Ti, Zr, Nb, Ta, W, etc [20,21].

3.2. Analysis of the interface between silicon and carbon substrate

In addition to tuning the polarization of the electrode by varying applied cell voltage or current density, the substrate also plays an important role in controlling the electrolytic Si products. Porous Si film could form on Ag substrate at various applied cell voltages, but it is not allowed to push the polarization to a more negative value because the Ca^{2+} could form low melting-point Ca–Ag alloy on Ag substrate. In comparison with the metal substrates, the interface between the Si deposit and carbon substrate could play a central role in guiding the growth of Si. However, no information could be found by XRD, SEM, and EDS analysis owing to their detection limitation if only a tiny product exists at the boundary. Fortunately, a dense film could form on graphite substrate (Fig. 3a), which is beneficial for investigating the interface between carbon and Si. From the cross-sectional SEM image of Si, a transition interlayer was observed (Fig. 3b–e), which could be due to the diffusion of C into Si or the formation of a layer of SiC (the electrolytic Si film was peeled off from the substrate before SEM test). The thickness of the transition layer is less than 1 μm, and the carbon concentration from the interface to the bulk gradually decreases (Fig. 3f). The surface of the Si film contacting with the molten salt electrolyte is rough and compact (Fig. 3g), which is pure Si verified by EDS analysis (Fig. 3h).

Thermodynamically, Si spontaneously reacts with carbon to generate SiC at 850 °C (Si + C = SiC, ΔG = −62.6 kJ/mol). However, the kinetics of the reaction is slow that SiC layer could be too thin to be detected by XRD, and XPS only detect the very surface of Si film. To obtain more chemical information from the interface, the XPS and TOF-SIMS analysis were employed together with a dynamic sputtering technique used to remove the surface of the sample step by step. Then the XPS signal was collected after different sputtering time. Before sputtering, SiO_2 layer was observed (Fig. 4a). Pure Si was observed after the SiO_2 layer was removed, and both elemental carbon and SiC information appeared after the sample was sputtered for 315 s. The XPS data confirm that the interlayer contains Si, SiC, and C [28]. The profile of TOF-SIMS signal tracing with sputtering time is shown in Fig. 4b. The boron and phosphorous contents are undetectable, which agrees well with the recently published data [29]. More importantly, the transition layer can be clearly detected using the sputtering-assisted characterization (Fig. 4b), agreeing with the XPS data that the transition layer contains Si, SiC, and C rather than a pure SiC layer. Since the carbon and silicon can diffuse into each side and only a partial carbon can react with silicon to form SiC. Unlike the reaction of Si with a metal substrate (e.g., Ni), the reaction kinetics of carbon and Si is slow at 850 °C. Thus, the transition layer between the Si and carbon is a mixture of Si, C, and SiC, which could reduce the tension between the Si and carbon substrate and the Si–C bonding could improve the adhesion of the Si film.

3.3. Electrochemical performance of Li-storage

Since the electrolytic Si layer has a rough surface and good connection with the carbon substrate, the Si film was applied as a binder-free anode in a lithium-ion battery. The reactivity of the Si film was characterized by cyclic voltammetry (Fig. 5a). The first reduction peak starts at 0.3 V *vs.* Li and the second peak appears at −0.1 V *vs.* Li. Upon the reverse scan, two symmetrical oxidation peaks corresponds to the dealloying processes of Li from the preformed Li–Si alloys. In the first cycle, the small redox peaks may be due to the reduction of SiO_2 layer formed in the air. The redox peaks increase with increasing scan number, indicating that the Si film was gradually activated or the surface area increased due to the swelling effect during the cycling. In a PEC test, the open circuit potential shifted to negative direction under irradiation, revealing that the obtained Si film is p-type (Fig. 5b). The variation of the potential is due to generated electrons move toward the p-type silicon surface in contact with the electrolyte, decreasing the open potential of the Si electrode. The dopants could help to increase the electronic conductivity of the electrolytic Si film and thereby be advantageous to increase the rate capability without adding the conductive additive. Without Si deposition, there is nearly no capacity coming from graphite substrate (Fig. 5c). The coulombic efficiency of the first five cycles is lower than 90%, which could be due to the growth of SEI and reduction of SiO_2 layer formed during posttreatment. For practical application, the initial coulombic efficiency should be further improved. The Si deposit (about 4 μm) delivers 2950, 2500, and 1950 mAh/g under a charge/discharge

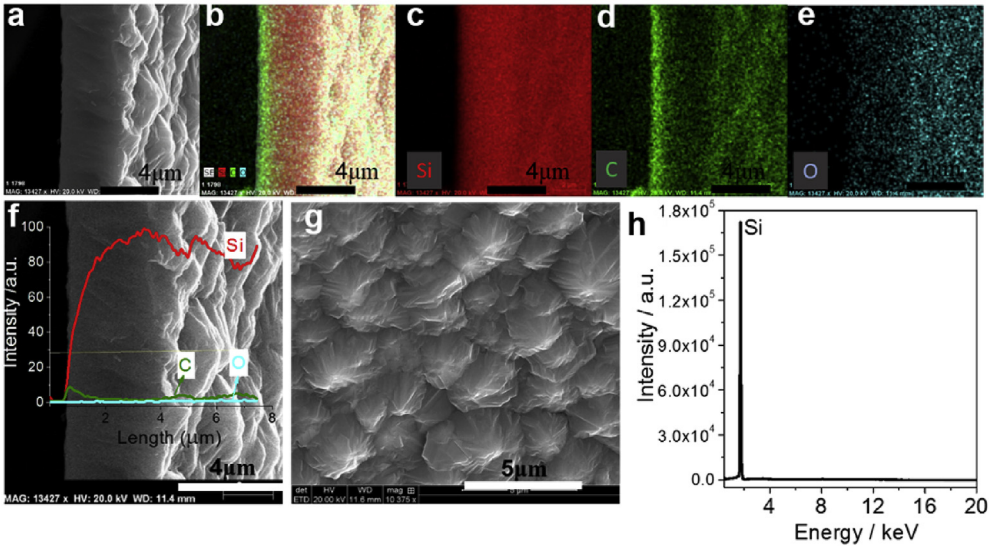

Fig. 3. SEM image (a) and its corresponding EDS mapping (b–e) of the electrolytic Si film (peeled off from the carbon substrate) including Si, C, O elements, linear element distribution profile (f), surface morphology (g), and EDS spectrum of the surface (h).

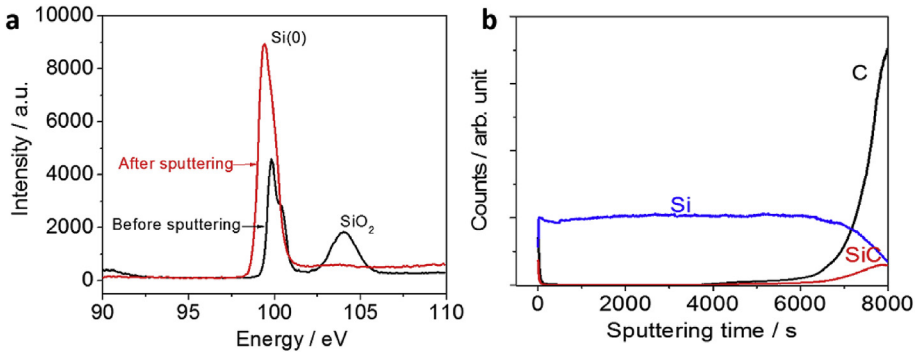

Fig. 4. XPS spectra of the Si film before and after sputtering (a); secondary ion mass spectroscopic depth profiles of the deposited Si film (b).

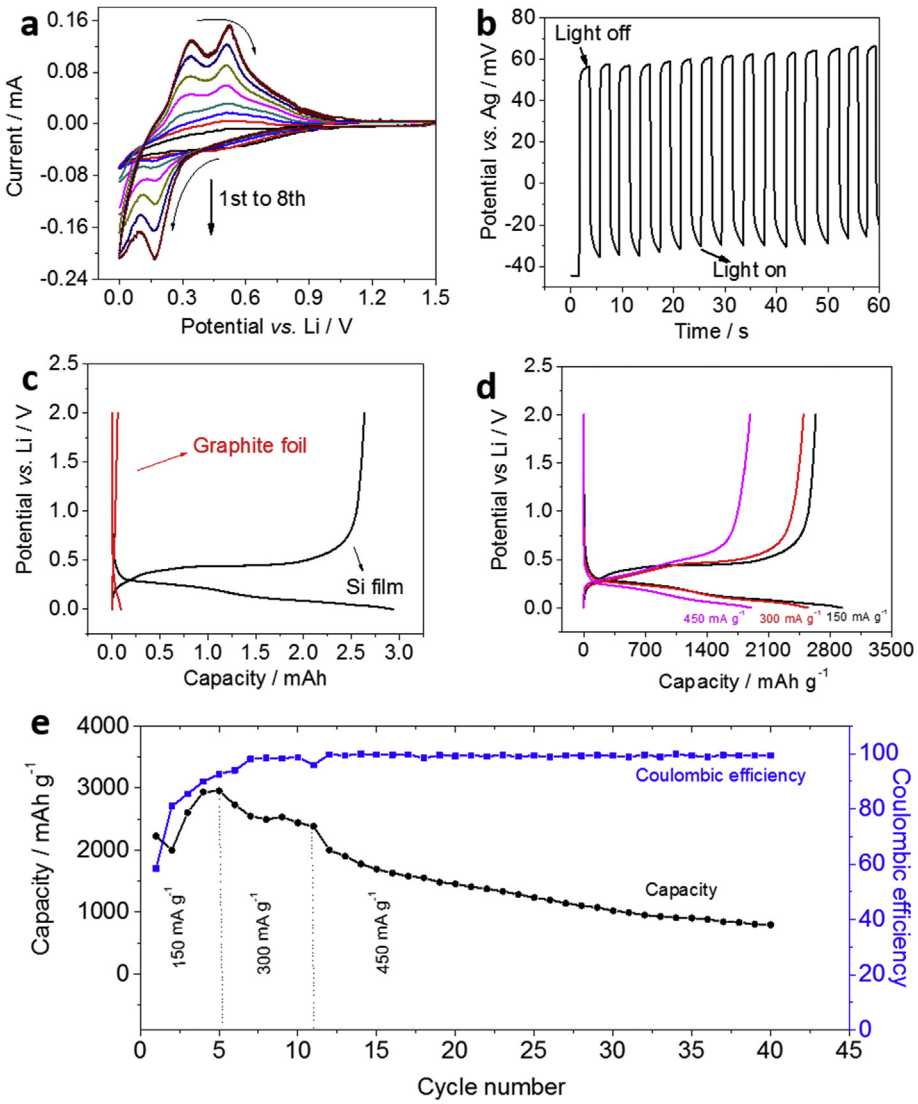

Fig. 5. (a) CVs of the Si deposit recorded at a scan rate of 0.025 mv s^{-1}; (b) potential response of the Si film varies with incident light; (c) capacities of a pure graphite foil with and without and Si film; (d) rate capabilities of Si film under indicated current densities; (e) cyclability test of the Si deposit.

current density of 150, 300, and 450 mA/g, respectively (Fig. 5d). Then the cyclability of Si deposit was investigated, and the retained capacity was 800 mAh/g after 40 cycles (Fig. 5e). As reported [36], the cyclability of Si film anode could be improved by decreasing of the thickness.

To apply this coating technology more broadly, the electrochemical coating of Si layer on carbon fibers was deployed. In the same electrolysis bath, the graphite substrate was replaced by carbon fibers with a diameter of 20 μm (Fig. 6). After being electrolyzed at 2.4 V for 2 h, a Si layer was coated on the surface of the

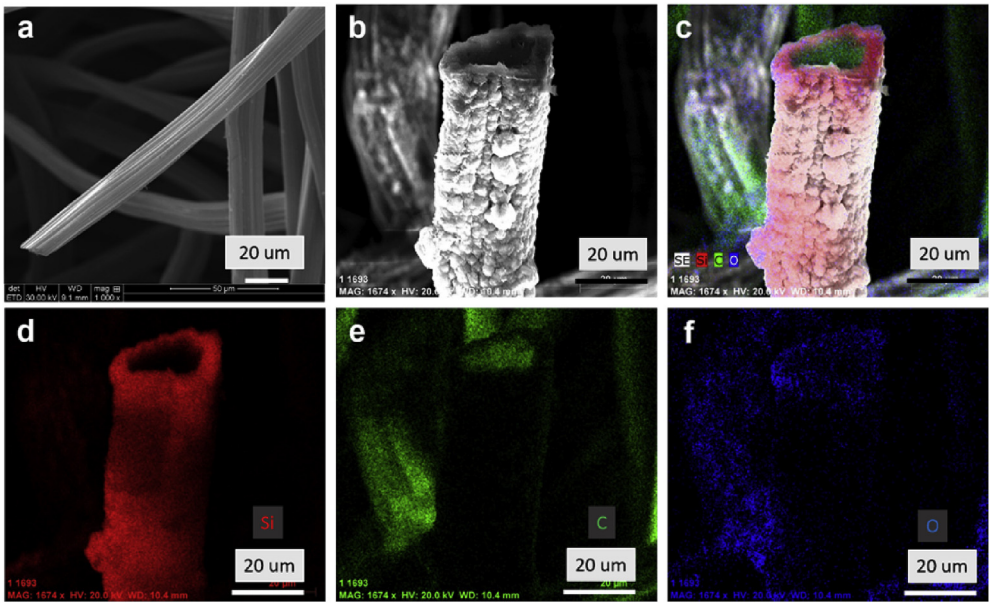

Fig. 6. SEM images of carbon fibers before (a) and after coated with Si film (b), (e–f) is their corresponding EDS mapping of Si, C, and O elements.

carbon fibers, forming a Si/carbon core-shell structure. Accordingly, this coating technology can be used for plating Si layer on various carbon materials with designed structures.

4. Conclusions

Electrochemical coating of Si film on both graphite foil and carbon fibers was achieved in molten $CaCl_2$–SiO_2 at 850 °C. On the graphite substrate, the morphologies of the Si deposit are controllable by controlling the applied cell voltage. Si nanowires of a diameter from 50 to 100 nm could be prepared under a cell voltage below 2.0 V. The Si deposit turns to a mixture of Si particles and wires under 2.2 V, and becomes a dense film under a cell voltage between 2.4 and 2.6 V. In addition to the applied cell voltage, the substrate plays an import role in assisting the growth of Si film. Using the XPS and TOF-SIMS analysis together with a dynamic sputtering method, a thin interlayer (<1 μm) consisting of Si, SiC and C ensures a good adhesion of Si film with the substrate. Rather than used for PEC applications, the p-type electrolytic Si film was first applied as a binder-free anode for LIBs delivering a capacity over 2500 mAh/g at 150 mA/g in first 10 cycles and retaining 800 mAh/g after 40 cycles. In addition to coating graphite foil, the electrochemical coating of Si on carbon fibers was accomplished in molten salt as well, suggesting that electrochemical coating technique could be a general approach to preparing Si deposits with controllable forms and Si/carbon core-shell structures for functional materials fabrication.

Acknowledgment

We thank the financial support from the National Science Foundation of China (NSFC, Grant No. 51704060, 51204039), National Thousand Talents Program of China, Postdoctoral Science Foundation from North University of China, and Global Climate and Energy Project (GCEP, Agreement No. 60853646-118146).

References

[1] V. Schmidt, J.V. Wittemann, U. Goesele, Thermodynamics, and electrical properties of silicon nanowires, Chem. Rev. 110 (2010) 361.
[2] D. Stüwe, D. Mager, D. Biro, J.G. Korvink, Inkjet technology for crystalline silicon photovoltaics, Adv. Mater. 27 (2015) 599.
[3] F. Priolo, T. Gregorkiewicz, M. Galli, T.F. Krauss, Silicon nanostructures for photonics and photovoltaics, Nat. Nanotechnol. 9 (2014) 19.
[4] K.Q. Peng, S.T. Lee, Silicon nanowires for photovoltaic solar energy conversion, Adv. Mater. 23 (2011) 198.
[5] A. Magasinki, P. Dixon, B. Hertzberg, A. Kvit, G. Yushin, High-performance lithium-ion anodes using a hierarchical bottom-up approach, Nat. Mater. 9 (2010) 353.
[6] N. Lin, Y. Han, J. Zhou, K.L. Zhang, T.J. Xu, Y.C. Zhu, Y.T. Qian, A low temperature molten salt process for aluminothermic reduction of silicon oxides to crystalline Si for Li-ion batteries, Energy Environ. Sci. 5 (2015) 3187.
[7] S. Ohara, J. Suzuki, K. Sekine, T. Takamura, Li insertion/extraction reaction at a Si film evaporated on a Ni foil, J. Power Sources 119 (2003) 591.
[8] U. Kasavajjula, C.S. Wang, A.J. Appleby, nano- and bulk-silicon-based insertion anodes for lithium-ion secondary cells, J. Power Sources 163 (2007) 1003.
[9] T. Munisamy, A.J. Bard, Electrodeposition of Si from organic solvents and studies related to initial stages of Si growth, Electrochim. Acta 55 (2010) 3797.
[10] J. Gu, E. Fahrenkrug, S. Maldonado, Direct electrodeposition of crystalline silicon at low temperatures, J. Am. Chem. Soc. 135 (2013) 1684.
[11] N. Borisenko, S.Z. Abedin, F. Endres, In situ STM investigation of gold reconstruction and of silicon electrodeposition on Au(111) in the room temperature ionic liquid 1-Butyl-1-methylpyrrolidinium bis(trifluoromethylsulfonyl) imide, J. Phys. Chem. B 110 (2006) 6250.
[12] U. Cohen, Some prospective applications of silicon electrodeposition from molten fluorides to solar cell fabrication, J. Electron. Mater. 6 (1977) 607.
[13] G.M. Rao, D. Elwell, R.S. Feigelson, Electrowinning of silicon from K_2SiF_6-Molten fluoride systems, J. Electrochem. Soc. 127 (1980) 1940.
[14] R. Boen, J. Bouteillon, The electrodeposition of silicon in fluoride melts, J. Appl. Electrochem. 13 (1983) 277.
[15] E.J. Frazer, B.J. Welch, A galvanostatic study of the electrolytic reduction silica in molten cryolite, Electrochim. Acta 22 (1977) 1179.
[16] G.M. Haarberg, L. Famiyeh, A.M. Martinez, K.S. Osen, Electrodeposition of silicon from fluoride melts, Electrochim. Acta 100 (2013) 226.
[17] K. Yasuda, K. Maeda, T. Nohira, R. Hagiwara, T. Homma, Silicon electrodeposition in water-soluble KF–KCl molten salt: optimization of electrolysis conditions at 923 K, J. Electrochem. Soc. 163 (2016) D95.
[18] K. Maeda, K. Yasuda, T. Nohira, R. Hagiwara, T. Homma, Silicon electrodeposition in water-soluble KF–KCl molten salt: investigations on the reduction of Si (IV) ions electrochemical/electroless deposition, J. Electrochem. Soc. 162 (2015) D444.
[19] G.Z. Chen, D.J. Fray, T.W. Farthing, Direct electrochemical reduction of titanium dioxide to titanium in molten calcium chloride, Nature 407 (2000) 361.
[20] A.M. Abdelkader, K.T. Kilby, A. Cox, D.J. Fray, DC voltammetry of electrodeoxidation of solid oxides, Chem. Rev. 113 (2013) 2863.
[21] W. Xiao, D. Wang, The electrochemical reduction processes of solid compounds in high temperature molten salts, Chem. Soc. Rev. 43 (2014) 3215.
[22] T. Nohira, K. Yasuda, Y. Ito, Pinpoint and bulk electrochemical reduction of insulating silicon dioxide to silicon, Nat. Mater. 2 (2003) 397.
[23] X.B. Jin, P. Gao, D.H. Wang, X.H. Hu, G.Z. Chen, Electrochemical preparation of silicon and its alloys from solid oxides in molten calcium chloride, Angew. Chem. Int. Ed. 43 (2004) 733.

[24] S.K. Cho, F.-R. Fan, A.J. Bard, formation of a silicon layer by electroreduction of SiO_2 nanoparticles in $CaCl_2$ molten salt, Electrochim. Acta 65 (2012) 57.
[25] W. Xiao, X. Jin, Y. Deng, D. Wang, X. Hu, G.Z. Chen, Electrochemically driven three-phase interlines into insulator compounds: electroreduction of solid SiO_2 in molten $CaCl_2$, ChemPhysChem 7 (2006) 1750.
[26] W. Xiao, X. Jin, G.Z. Chen, up-scalable and controllable electrolytic production of photo-responsive nanostructured silicon, J. Mater. Chem. A 1 (2013) 10243.
[27] S.K. Cho, F.-R. Fan, A.J. Bard, Electrodeposition of crystalline and photoactive silicon directly from silicon dioxide nanoparticles in molten $CaCl_2$, Angew. Chem. Int. Ed. 51 (2012) 12740.
[28] J. Zhao, H.Y. Yin, T. Lim, H.W. Xie, H.-Y. Hsu, F. Forouzan, A.J. Bard, Electrodeposition of photoactive silicon films for low-cost solar cells, J. Electrochem. Soc. 163 (2016) D514.
[29] X. Yang, L. Ji, X.L. Zou, T. Lim, J. Zhao, E.T. Yu, A.J. Bard, Toward cost-effective manufacturing of silicon solar cells: electrodeposition of high-quality Si films in a $CaCl_2$ -based molten salt, Angew. Chem. Int. Ed. 56 (2017) 15078.
[30] W. Xiao, X. Wang, H.Y. Yin, H. Zhu, X.H. Mao, D.H. Wang, Verification and implications of the dissolution–electrodeposition process during the electroreduction of solid silica in molten $CaCl_2$, RSC Adv. 2 (2012) 7588.
[31] Y. Dong, T. Slade, M.J. Stolt, S.N. Girard, L.Q. Mai, S. Jin, Low temperature molten salt production of silicon nanowires by electrochemical reduction of $CaSiO_3$, Angew. Chem. Int. Ed. 56 (2017) 201707064.
[32] W. Xiao, J. Zhou, L. Yu, D.H. Wang, X.W. Lou, Electrolytic formation of crystalline silicon/germanium alloy nanotubes and hollow particles with enhanced lithium-storage properties, Angew. Chem. Int. Ed. 55 (2016) 7427.
[33] H.Y. Yin, W. Xiao, X.H. Mao, W.F. Wei, H. Zhu, D.H. Wang, Template-free electrosynthesis of crystalline germanium nanowires from solid germanium oxide in molten $CaCl_2$–NaCl, Eelctrochim. Acta 102 (2013) 369.
[34] X.L. Zou, L. Ji, X.G. Lu, Z.F. Zou, Facile electrosynthesis of silicon carbide nanowires from silica/carbon precursors in molten salt, Sci. Rep. (2017), https://doi.org/10.1038/s41598-017-10587-5.
[35] X.L. Zou, L. Ji, X. Yang, T. Lim, E.T. Yu, A.J. Bard, Electrochemical formation of a p-n junction on thin film silicon deposited in molten salt, J. Am. Chem. Soc. 139 (2017) 16060.
[36] M. Uehara, J. Suzuki, K. Tamura, K. Sekine, T. Takamura, Evaluation of the Li insertion/extraction reaction rate at a vacuum-deposited silicon film anode, J. Power Sources 146 (2005) 445.